

FINITE-ELEMENT MODELLING OF THE CONSERVATION EFFECTS OF AN ARTIFICIAL RESIN ON DETERIORATED HETEROGENEOUS SANDSTONE IN BUILDING RESTORATION.

FINITE-ELEMENT MODELLIERUNG DES EINFLUSSES VON KUNSTHARZBEHANDLUNGEN AUF NATURSTEIN IN DER KONSERVIERUNG VON BAUDENKMÄLERN AM BEISPIEL EINES VERWITTERTEN, HETEROGENEN SANDSTEINS.

MODELISATION PAR ELEMENTS FINIS DES EFFETS DE CONSERVATION D'UNE RESINE ARTIFICIELLE SUR GRES HETEROGENE DETERIORE.

J. Bossert¹, J. Ožbolt¹ and G. Grassegger²

¹Institute of Construction Materials, University of Stuttgart, Germany

²Otto-Graf-Institut - Research and Testing Establishment for Materials and Structures, Department 32 - Maintenance and Restoration of Historical Monuments, University of Stuttgart, Germany

ABSTRACT

Besides experimental investigations related to the strengthening effects of resins to natural stone, there have been hardly any numerical simulations conducted to the effects of the conservation on the mechanical behaviour of conserved objects. In the present study a three-dimensional finite element code MASA was used to investigate the influence of the conservation procedure on the mechanical properties of the natural stone. The finite element code is based on the microplane material model. As a localization limiter the crack band method was used. A typical profile of sandstone resembling parts of a sculpture - with scaling, sandy decay and sound zones was discretized by a solid finite elements. Varied were material properties, temperature distribution over the depth of the specimen, cyclic effects due to the temperature variation and geometry of the specimen. Numerical results show that as a consequence of change of material properties after conservation procedure the cracks can be generated under environmental conditions that are most likely possible in the

practice. This is especially true for extreme temperature gradients, for repeated temperature conditions (cyclic loading) and for complex geometries. Regular temperature impact, like normal weather cycles, did not cause any risk of high tensions or ruptures. Also continuous material properties were not endangered by high tensile stresses. The numerical results have been partly verified by experiments.

ZUSAMENFASSUNG

An kunstharzgetränkten Steinobjekten liegen nur sehr wenige theoretische oder mechanische Berechnungen zur Auswirkung der Harzfestigungen vor, die häufig als Konservierungsmethode eingesetzt werden. Es wurden in der Regel nur experimentelle Kennwerte ermittelt. Aus diesem Grunde wurde mit dem FE-Programm MASA der Einfluß von porenfüllenden Kunstharzbehandlungen auf Naturstein, aufbauend auf mechanische Literaturwerte und eigene Messdaten für einen Mustersandstein berechnet. Das FE-Programm baut auf dem „Microplane“ Modell auf und nutzt den Ansatz der verschmierten Risse. Hierfür wurden als geometrische Randbedingungen ein typisches Segment aus einer geschädigten Skulptur verwendet, das als Schädigungsprofil Schalenbildung, Absanden, Risse usw. bis hin zum gesunden Kern aufwies. Dieses wurde in FE-Elemente mit jeweils unterschiedlichen Materialeigenschaften, auf Grund der unterschiedlichen Schädigung und des Harzanteils, zerlegt. Variiert wurden dann äußere Belastungen wie Temperatureinfluß und Temperaturwechsel, die mechanischen Mischeigenschaften des „Verbundstoffes“, sowie die geometrischen Randbedingungen, bis hin zu stark gegliederten Oberflächen mit einspringender Geometrie. Die Ergebnisse der ersten Berechnungen zeigen, daß bei sehr großen Materialheterogenitäten, hier speziell bei Rißfüllungen mit Harz und sehr ungünstigen Klimabedingungen, wie extreme Temperaturwechsel, Spitzenspannungen bis zu Rissen auftreten könnten. Weitere Schwachstellen sind komplexe, feingliedrige Geometrien und vermutlich häufige klimatische Wechselbelastungen. Bei normalen Temperaturbelastungen und fließenden Übergängen von Eigenschaften waren keine Probleme zu beobachten.

RESUME

A ce jour, très peu de simulations numériques des effets de consolidation des résines artificielles utilisées pour conserver la pierre naturelle ont été réalisées. En général, les études étaient de nature expérimentale. Dans l'étude pré-

sente, le logiciel « MASA » et un maillage tridimensionnel ont été utilisés pour analyser l'influence de la procédure de conservation sur les propriétés physiques de la pierre naturelle. Le code des éléments finis est basé sur le modèle « microplane ». Un segment typique d'une sculpture traitée avec une résine acrylique et contenant zones saines, écaillages, fissures et désagrégation sableuse a été discrétisé avec des éléments finis solides. Les propriétés mécaniques du matériau, la distribution de température, les variations de température et la géométrie ont été variées. Les résultats montrent que de fortes inhomogénéités, comme par exemple les fissures remplies de résines, peuvent, sous des conditions climatiques défavorables, être le lieu de pics de tension, voire de nouvelles fissures. Dans des conditions thermiques normales et sans changement abrupt des propriétés mécaniques du matériau, ces pics de tension et l'endommagement en résultant n'ont pas lieu. Une géométrie très filigrane, des gradients de température extrêmes et une résine très rigide sont particulièrement critiques. Les résultats numériques ont partiellement été confirmés par des essais.

INTRODUCTION

All masonry materials and especially building stones undergo aging and deterioration processes. A rather new method, which has been in last 20 years used for conservation of precious sculptures and structural parts, is an impregnation procedure by using acrylic resin monomers in special designed treatment equipment, performed by a restoration company. It has saved many distressed and offers the possibility to place them back at their original architectural surrounding. The resin penetrates in the predried objects completely and polymerises in the pore space with only minimal shrinkage. The preservation treatment is very good because the internal stone surface is completely covered by stable resin films. The resin consolidant has been investigated in many ways, however, it was not investigated as a part of a composite which consists of materials that have rather different mechanical and hydro-thermal properties.

In general, the consolidation treatment leads to the following change of properties: increase of tensile strength, increase of elastic modulus, different thermal conductivity and heat capacity, reduction of porosity almost to zero and reduction of moisture expansion properties (swelling).

The problem is that in spite of the increase of the strength after the conservation some cases of damage were reported. Furthermore, the mechanical

change of properties of the consolidated stone were of general interest. Therefore, the numerically investigated influence of the conservation procedure on the structural behaviour of the treated sandstone is reported here. The proposed model used for the finite-element simulations is a typical profile of decaying and scaling sandstone object (see Fig. 1).



Fig. 1 Typical deterioration of sandstones scaling on the surface and beneath it sandy decay

After the treatment with resin this profile of sandstone will, as an extreme case, be a quasi-multilayered structure with different percentages of resin in pore space and will possess different mechanical properties within each layer (4) (see Fig. 2). The plotted line indicates the loss of strength, from very low in the crack zone under the scale to 100 % in the core. The model consists of the surface scale A (weaker than the natural stone but still stable), a layer B which is brittle to sandy decaying but still connected to the scale, the crack zone C with highly increased porosity and up to 100 % resin in cracks. The next zone is the sandy to brittle transition zone D with increasing stiffness and finally the sound core E. The main assumption is that the strength of each layer is related to its porosity.

Initially, the change of the material properties caused by the treatment by artificial resin was investigated. Because of a lack of the characteristic values of a treated sandstone at different porosities a simple model to estimate these properties of the composite (sandstone – artificial resin) was proposed. This model, being closely related to homogenisation concepts in continuum mechanics, uses the material properties of the components and their volume fraction to estimate

the effective (macroscopic) properties of the composite. For the sandstone we used the technical properties of the “Schilfsandstone” a common Keuper fine sandstone from Baden-Württemberg consisting of a large portion of a rock fragments besides quartz, feldspar, cemented by feldspar and chlorite cements with an average porosity of 17 % by volume (3).

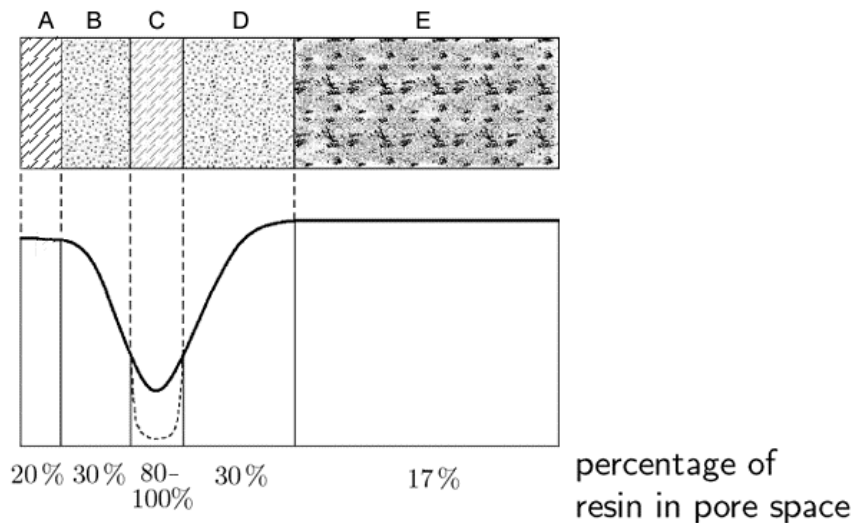


Figure 2 The distribution quantities of resin (percentage) in the pore space within the former deteriorated scaling zone. Profile from the outside weathering zone (left) to the sound core (right). Plotted line indicates the loss of strength because of weathering.

We calculated the physical properties by averaging the Reuss- and Voigt-approaches (1). In the one-dimensional case these two approximations can simply be imagined to be as shown in Fig. 3 and Fig. 4.

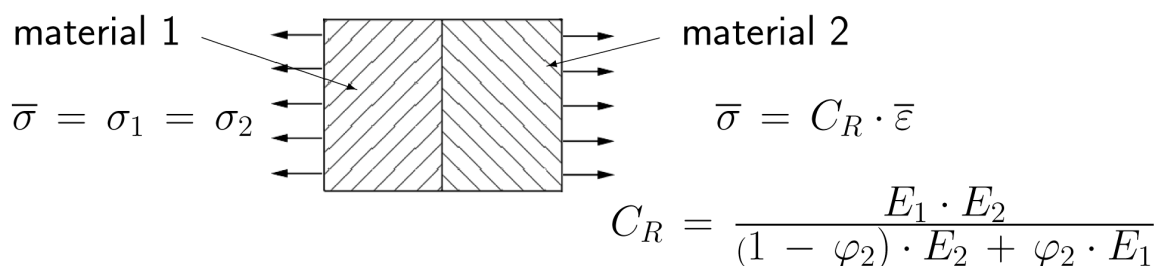


Figure 3 Homogenisation model of the material - Reuss-approximation (The stresses over the cross-section of the two materials are equal and constant).

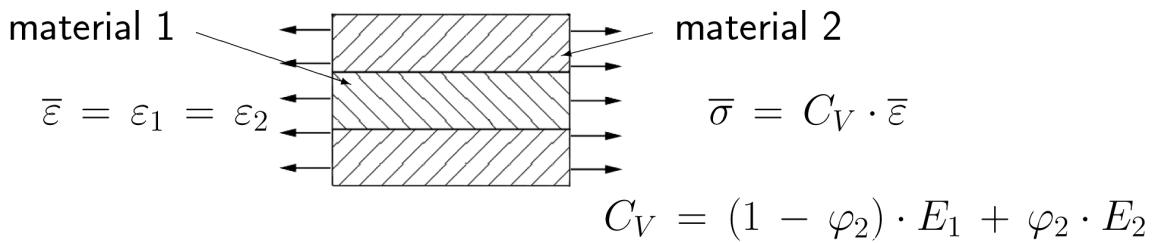


Figure 4 Homogenisation model of the material - Voigt-approximation (The strains over the cross-section of the two materials are equal and constant).

It has been demonstrated that these values represent the real lower and upper bounds of the elastic modulus of composite materials with elastic behaviour. The homogenisation procedure is schematically shown in Fig. 5.

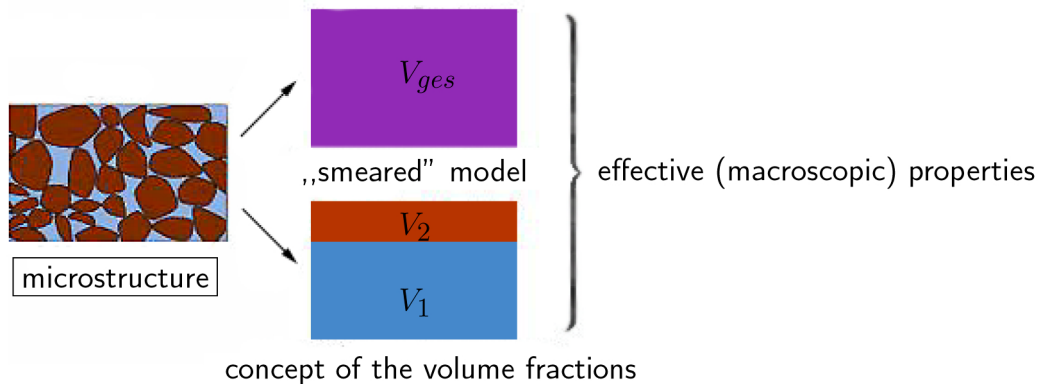


Figure 5 Effective macroscopic properties of composite material.

The physical properties from our model were partly verified by experiments and partly by the values from the literature or former investigations. Examples for the approximation of the tensile strength, the elastic modulus and the coefficient of thermal expansion are shown in Figs. 6, 7 and 8. After the initial calculation, the experimental data were used to adjust the starting values for the final calculation.

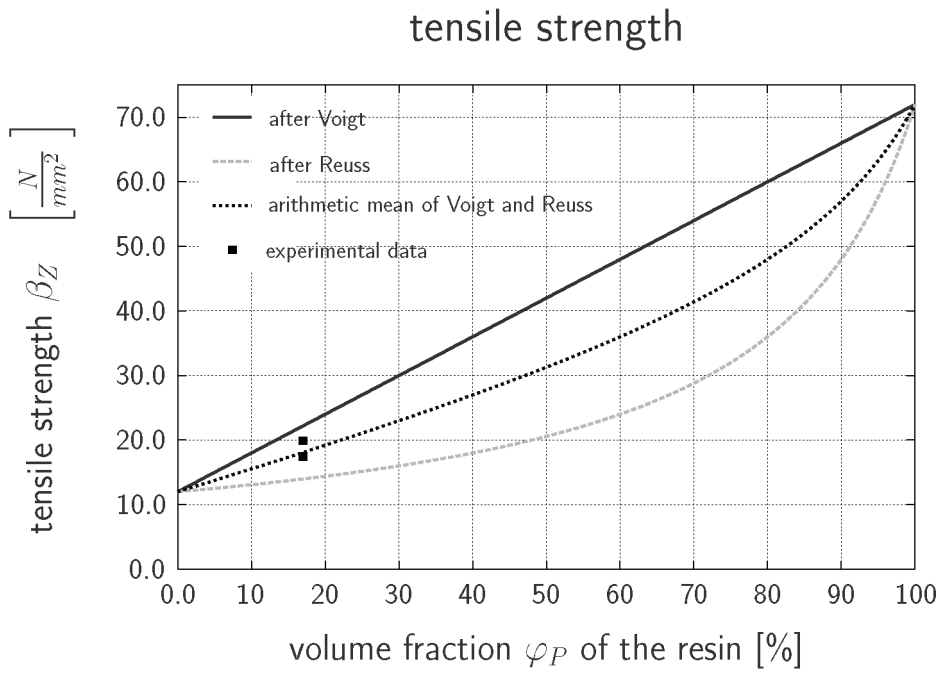


Figure 6 Homogenisation of the compound materials theoretic approaches and experimental verification - the dependence between tensile strength and percentage of resin.

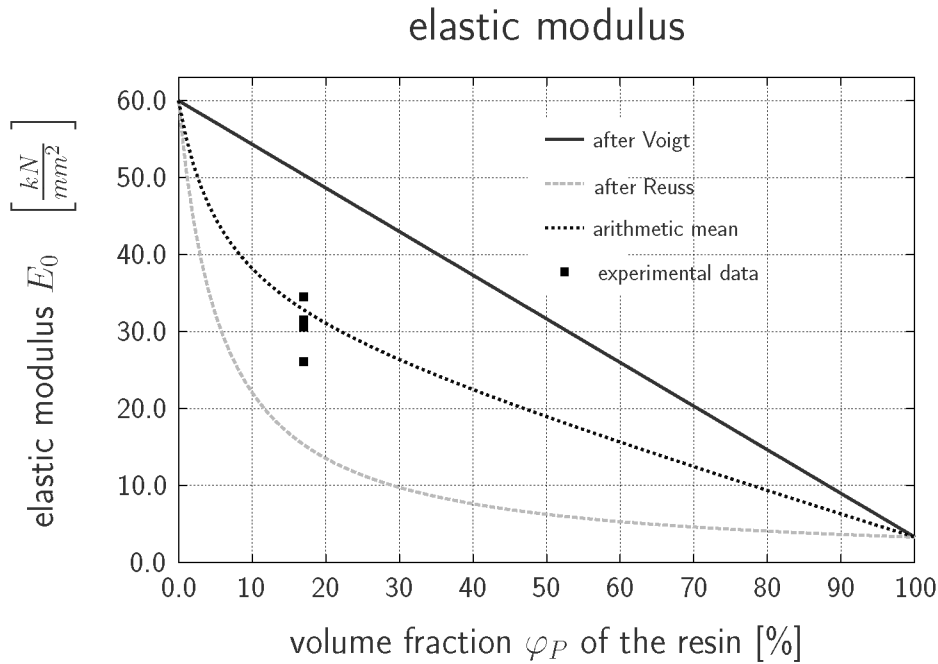


Figure 7 Homogenisation of the compound materials theoretic approaches and experimental verification - the dependence between elastic modulus and percentage of resin.

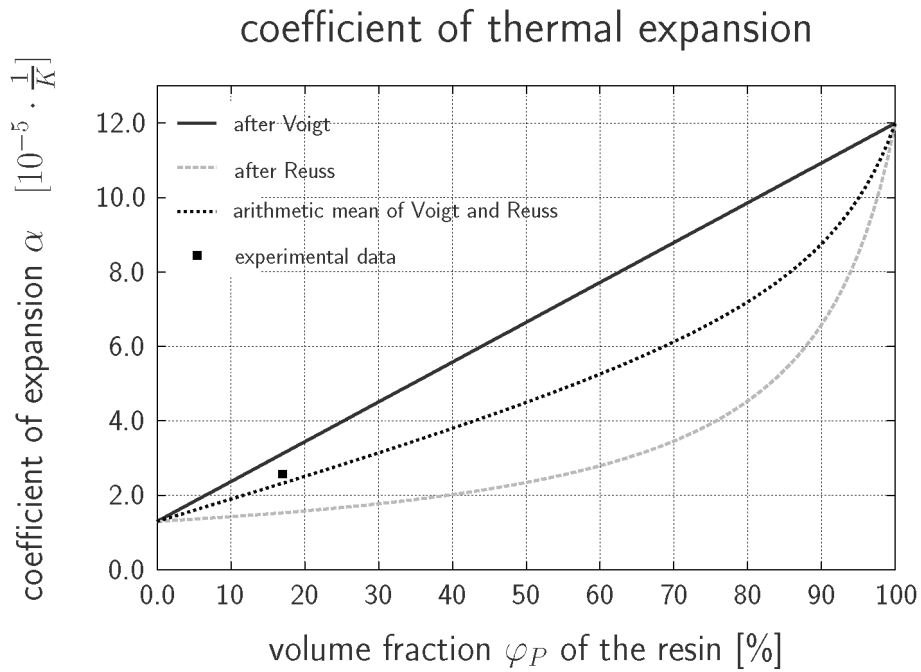


Figure 8 Homogenisation of the compound materials theoretic approaches and experimental verification - the dependence between coefficient of thermal expansion percentage of resin.

Summary of the calculated material properties for different porosities is given in Table 1.

Table 1 Calculated material properties for different porosities according to the homogenisation theories.

volume fraction of resin φ_{resin}	[%]	17.0	20.0	30.0	80.0	100.0
tensile strength β_Z	$[N/mm^2]$	18.5	19.6	23.5	48.5	72.0
compressive strength β_D	$[N/mm^2]$	57.0	59.0	64.0	94.0	110.0
elastic modulus E_0	$[kN/mm^2]$	33.5	31.5	26.7	9.4	3.3
poisson's ratio ν	$[-]$	0.11	0.12	0.14	0.25	0.40
coefficient of thermal expansion α_T	$[\cdot 10^{-5}/K]$	2.3	2.5	3.2	7.2	10.0
heat capacity c_P	$[kJ/kgK]$	1.03	1.04	1.09	1.37	1.50
thermal conductivity λ	$[W/mK]$	1.3	1.2	0.9	0.3	0.18
density ρ_0	$[t/m^3]$	2.40	2.35	2.20	1.47	1.18

The results shown in the Figs. 6-8 were experimentally verified on 3-4 impregnated samples of the Schilfsandstone. The experimental results show good agreement with the calculated values of the homogenisation theories. The elastic modulus has also been measured (see Fig. 7) and it shows relatively good agreement with the predicted values. The experimental verification is also shown in Fig. 9a to 9c (3). The impregnated material reveals a much higher modulus of elasticity and a brittle fracture at much higher tensile stresses.

EXPERIMENTAL VERIFICATION

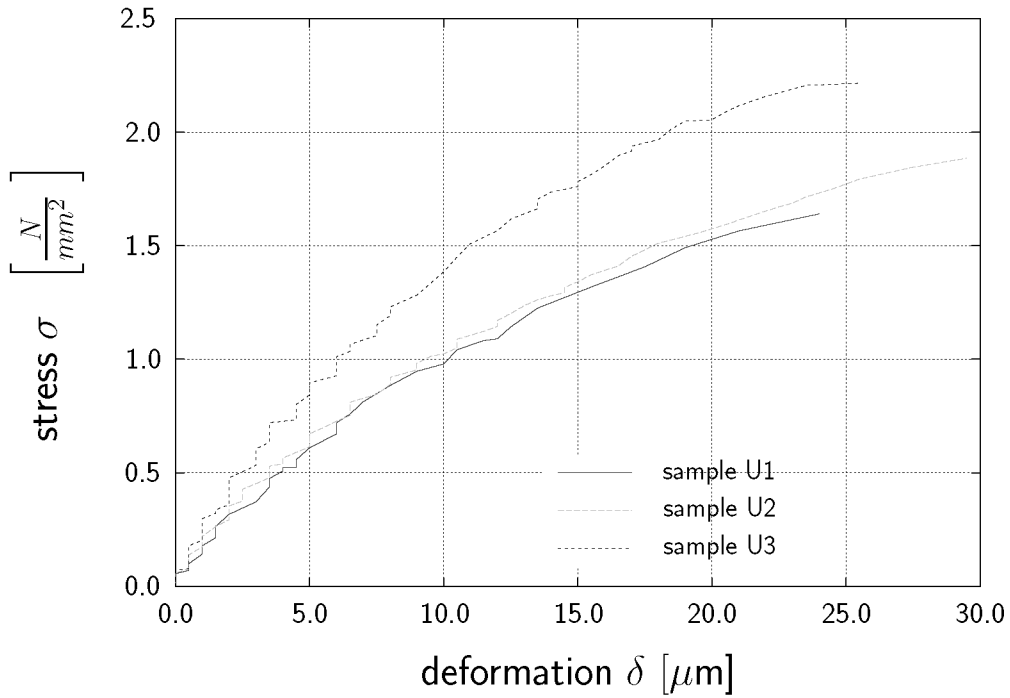


Figure 9a Stress-displacement-curve of three different samples of sound Schilfsandstone (untreated). Results of a centric tension test of prismatic samples with a diameter of 5 cm and length of 15 cm.

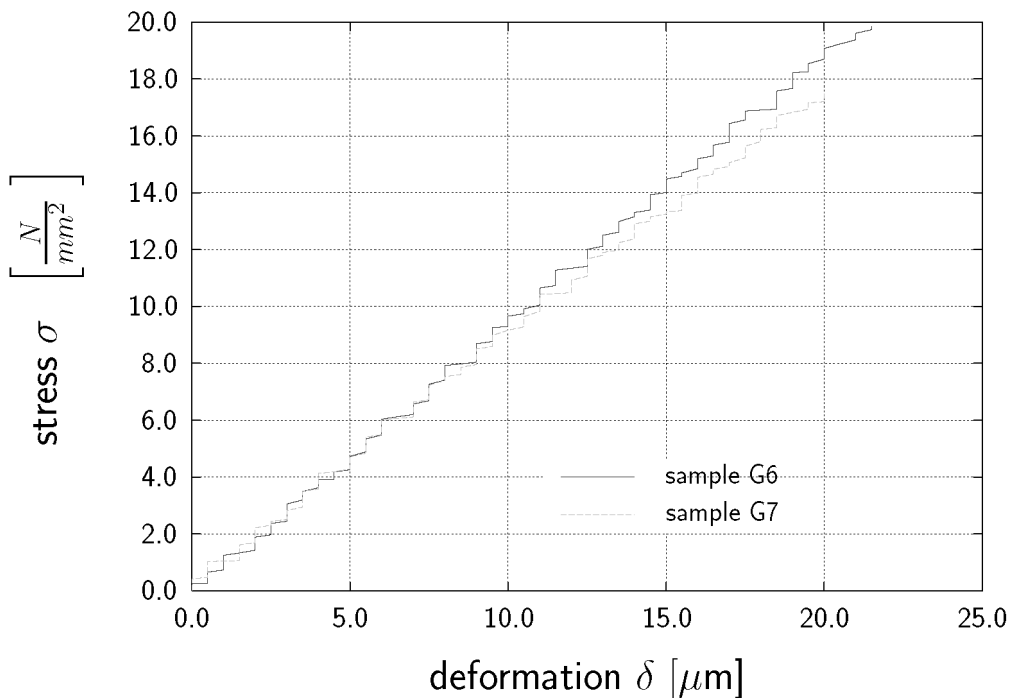


Figure 9b Stress-displacement-curve of two different samples of sound Schilfsandstone completely impregnated by resin. Results of a centric tension test of prismatic specimen with a diameter of 5 cm and length of 15 cm.

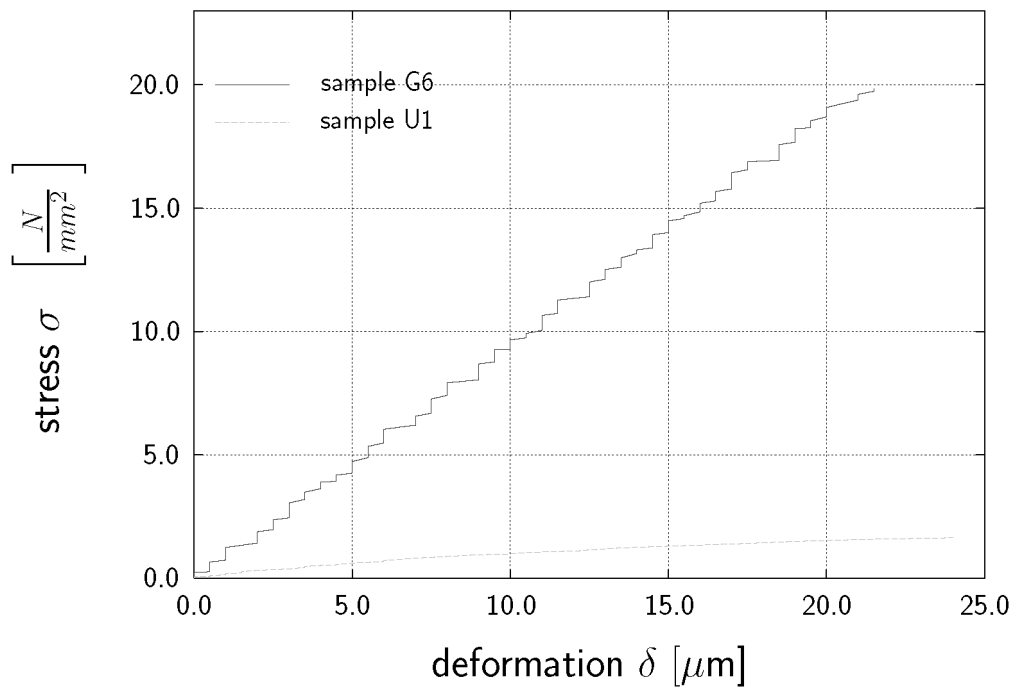


Figure 9c Comparison of stress-displacement-curves of two different samples of Schilfsandstone specimen g is completely impregnated by resin and specimen u untreated. Results of a centric tension test of prismatic specimen with a diameter of 5 cm and length of 15 cm.

MODELLING

The proposed geometry of the model and boundary conditions were chosen such that they resemble parts of a sculpture like an arm of a statue or a detail of a balustrade (see Fig. 10). For the FE-simulations the model was discretized by four-node 3D elements, whereas different material properties were discretized by the layers of finite elements. Figure 10 shows the FE-model, a section of a semi-cylinder, exploiting the symmetry conditions. The marked layer is the intermediate layer (layer C in fig. 2) consisting of almost 100% resin (compare Fig. 2). From the mechanical point of view in the initial state of modelling each layer of the material is assumed to be isotropic.

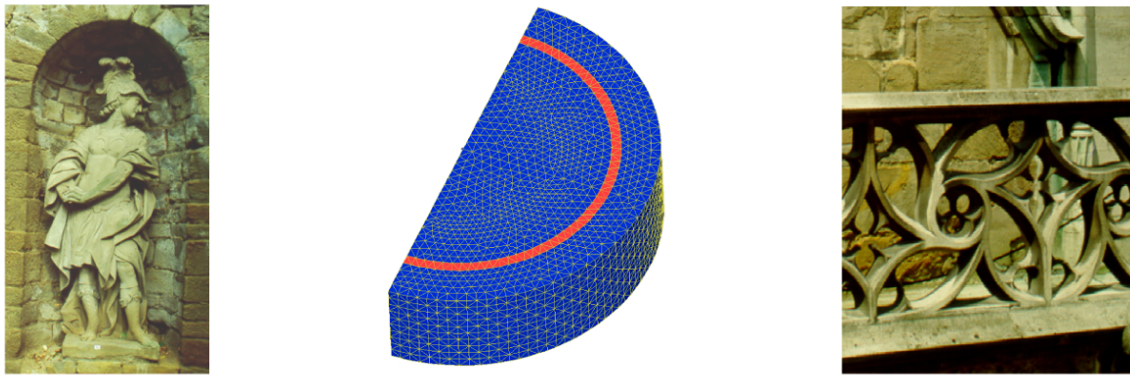


Figure 10 Three-dimensional finite element discretization of structural parts – layered approach

The model of layers, as an approximation of the consolidated sandstone, consists of the layers like proposed in Fig. 2. It consists of the surface scale (weaker than the natural stone but still stable), a layer which is brittle to sandy decay but still connected to the scale, a crack zone, a second sandy decay zone with increasing stiffness and a gradual change towards sound stone, called zones A to D. It has to be pointed out, that after impregnation the strength of the profile is completely changed, because of the rather high strength of the resin and the variation of the percentage of resin.

NUMERICAL ANALYSIS

The three-dimensional FE-analysis consists of two parts: calculation of thermal loading and calculation of stresses and strains.

Because of the treated sandstone being fully saturated with resin there are no more chemical or moisture influences, e.g. like moisture expansions. The eigenstresses due to the polymerisation and shrinkage of the resin were not considered because they degrade with time (relaxation). Besides external causes like dead or working loads (as normally also regarded in structural analysis) have been also neglected in the present study.

THERMAL LOADING

The following climatic effects were taken into account. Time dependent thermal influences (air temperature, direct and indirect solar radiation, precipitation) lead to the different transient temperature distributions. They were calculated using the finite-element-method by approximating the solution by the

weak form of the Fourier differential-equation with different boundary conditions. The applied numerical solution is based on the Crank-Nicolson-method (8), (9).

From physics-of-construction references, 8 cases of extreme climate situations sometimes occurring in Germany were chosen for the modelling of extreme temperature load (7). Initially, it has been shown that the regular temperature variations of the climate have no critical impact. However, there are several critical temperature loads. Besides the loading cases “warming-up” and “cooling down” in summer and winter, respectively, the cases “thunder shower in summer” – which simulates (cold) rainfall on a warmed surface were also considered. They leads to extreme temperature distributions. Figures 11 and 12 show this extreme temperature situation which were calculated for two different specimen profiles.

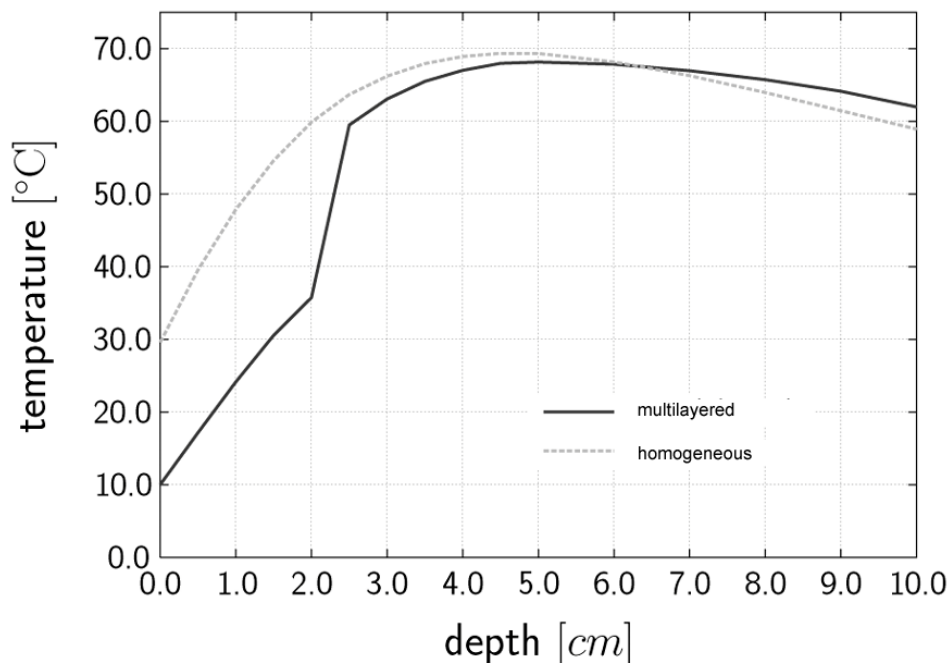


Figure 11 Temperature distribution caused by “thunder-shower”.

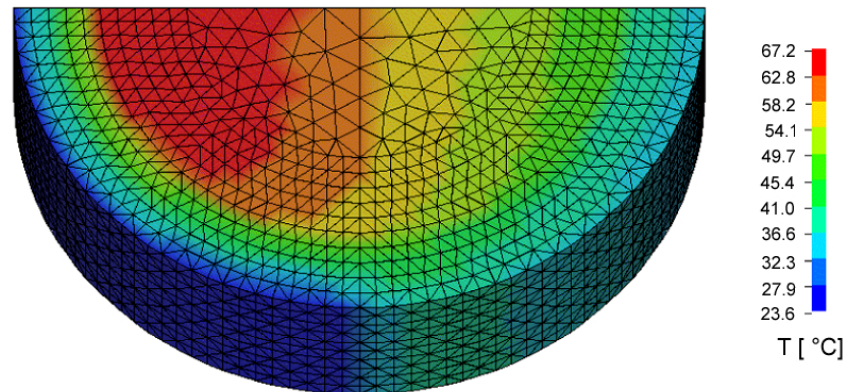


Figure 12 Temperature distribution caused by “thunder-shower” with indirect radiation from the right side and direct and indirect radiation from the left side.

It can be seen that because of the multilayered structure and the low thermal conductivity of the intermediate resin layer an extreme gradient occurs. In comparison to the homogeneous profile (no layers of different materials) the temperature on the surface of the multilayered geometry is much lower.

CALCULATION OF STRESS AND STRAIN DISTRIBUTION

The finite element code MASA (5) employed in the present study can be used for the non-linear finite element (FE) analysis of quasi-brittle (concrete-like) materials. It is based on the microplane material model and the smeared crack concept. As a regularization procedure the crack band approach is used (2).

To calculate distribution of stresses and strains one needs the material constitutive law. Here, the microplane model is used. The microplane model (6) is characterized by a relation between the stress and strain components on planes of various orientations. These planes may be imagined to represent the damage planes or weak planes in the microstructure, such as contact layers between aggregates in concrete. In the model the tensorial invariance restrictions need not to be directly enforced. Superimposing the responses from all microplanes in a suitable manner automatically satisfies them.

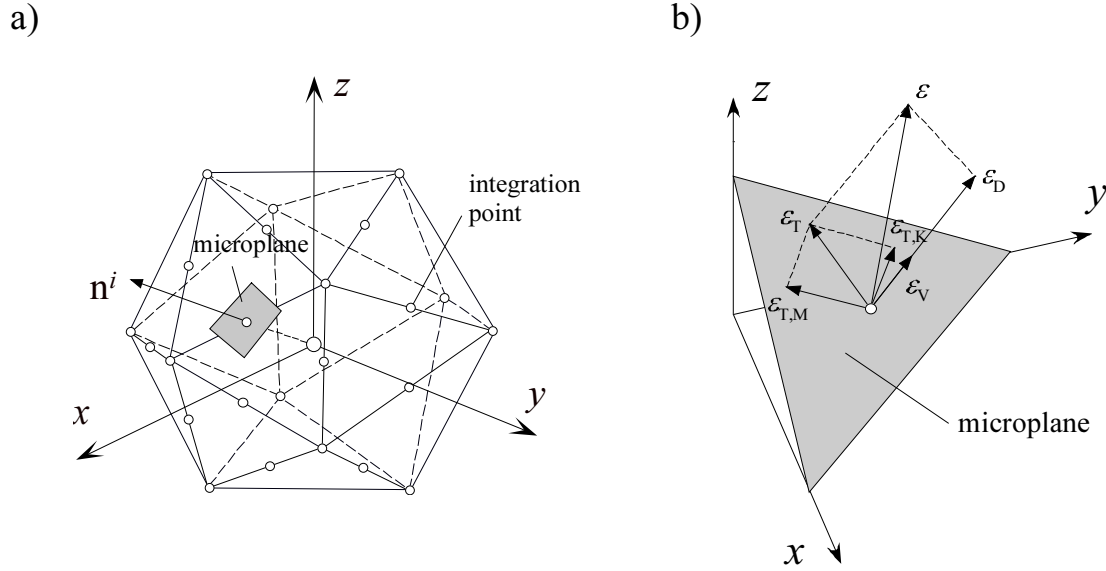


Figure 13 The concept of the microplane model: a) discretization of the unit volume sphere for each finite element integration point (21 microplane directions) and b) microplane strain components.

The recently proposed version of the microplane model for “concrete materials” is based on the so-called relaxed kinematic constraint concept (6). In the model the microplane (see Fig. 13) is defined by its unit normal vector of components n_i . Normal and shear stress and strain components (σ_N , σ_{Tr} , ϵ_N , ϵ_{Tr}) are considered on each plane. Microplane strains are assumed to be the projections of the macroscopic strain tensor ϵ_{ij} (kinematic constraint). Based on the virtual work approach, the macroscopic stress tensor is obtained as an integral over all possible, in predefined, microplane orientations (Ω denotes the surface of the unit sphere):

$$\sigma_{ij} = \frac{3}{2\pi} \int_{\Omega} \sigma_N n_i n_j d\Omega + \frac{3}{2\pi} \int_{\Omega} \frac{\sigma_{Tr}}{2} (n_i \delta_{ij} + n_j \delta_{ii}) d\Omega \quad (1)$$

To realistically model quasi-brittle materials, the normal microplane stress and strain components have to be decomposed into the volumetric and deviatoric parts ($\sigma_N = \sigma_V + \sigma_D$, $\epsilon_N = \epsilon_V + \epsilon_D$; see Figure 13), what leads to the following expression for the macroscopic stress tensor:

$$\sigma_{ij} = \sigma_V \delta_{ij} + \frac{3}{2\pi} \int_{\Omega} \sigma_D n_i n_j d\Omega + \frac{3}{2\pi} \int_{\Omega} \frac{\sigma_{Tr}}{2} (n_i \delta_{rj} + n_j \delta_{ri}) d\Omega \quad (2)$$

For each microplane component, the uniaxial stress-strain relations are assumed as:

$$\sigma_V = F_V(\varepsilon_{V,eff}) \quad ; \quad \sigma_D = F_D(\varepsilon_{D,eff}) \quad ; \quad \sigma_{Tr} = F_{Tr}(\varepsilon_{Tr,eff}) \quad (3)$$

where F_V , F_D and F_{Tr} are the uniaxial stress-strain relationships for volumetric, deviatoric and shear components, respectively. From known macroscopic strain tensor, the microplane strains are calculated based on the kinematic constraint approach. Finally, the macroscopic stress tensor is obtained from (2). The integration over all microplane directions (21 directions) is performed numerically.

The basic mechanical properties that are needed for the non-linear smeared fracture finite element analysis are Young's modulus, Poisson's ratio, uniaxial tensile and compressive strength and fracture energy. For each layer of the material these properties are obtained from the literature or from the experiments. In our case it was calculated as shown above (see Tab. 1) and verified by experiments.

The results of the stress and strain calculation show that extreme loads can cause stresses in the range of the tensile strength. For the extreme loading case, i.e. the "thundershower", the stress and strain distributions are plotted in Fig. 14. Figure 15 shows the stress distribution over the depth of the FE-model.

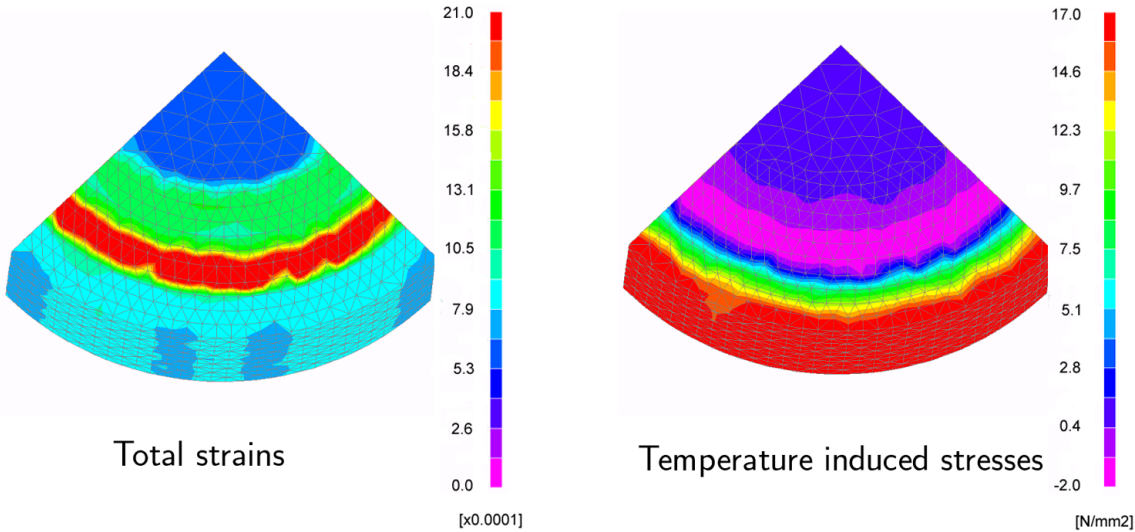


Figure 14 Calculated distribution of stresses and strains for the temperature distribution caused by “thunder-shower” (mainly in tangential direction).

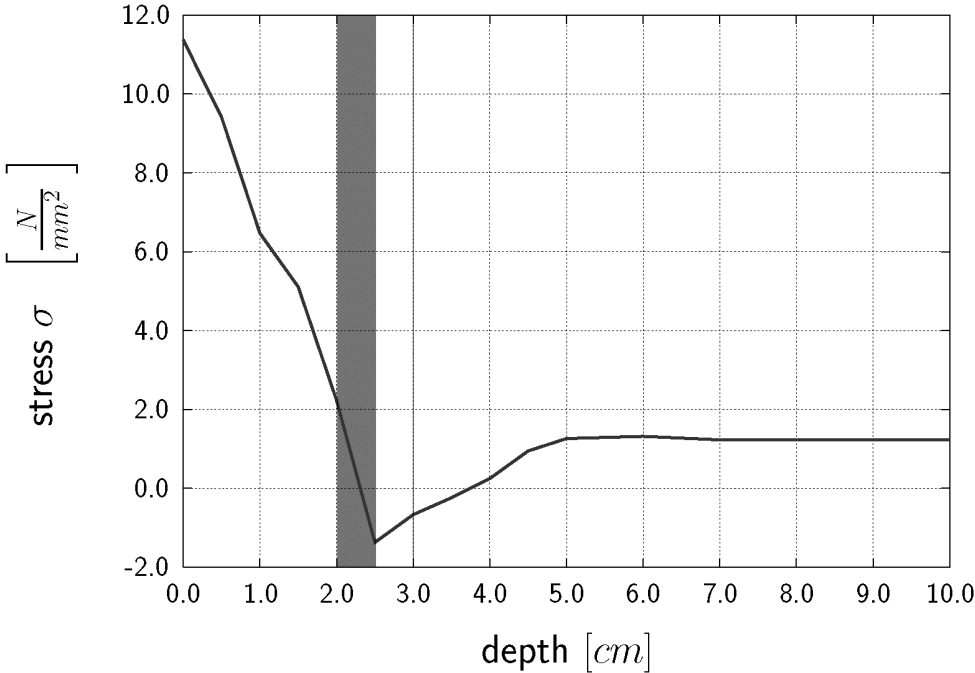


Figure 15 Calculated distribution of stresses at a chosen section over the depth of the model for the temperature distribution caused by “thunder-shower” (blue = layer consists of 100% resin).

The zone marked blue is the intermediate layer C consisting of 100% resin. The plot of the total strains shows that there is a highly expanding layer in radial direction. This occurs in the intermediate resin layer C. The corresponding stresses for this loading case are rather high, especially on the surface. This is a consequence of the incompatibility between the thermal expansions of the different layers next to the surface.

In order to investigate the consequence of several reference temperatures (that is the temperature of stress-free state of the material), initially for the calculations the reference temperature was set to $T=25^{\circ}\text{C}$. In additional calculations this temperature was varied. The resulting plots shown in Fig. 16 demonstrate that the influence of the reference temperature can in this special case be neglected with sufficient accuracy.

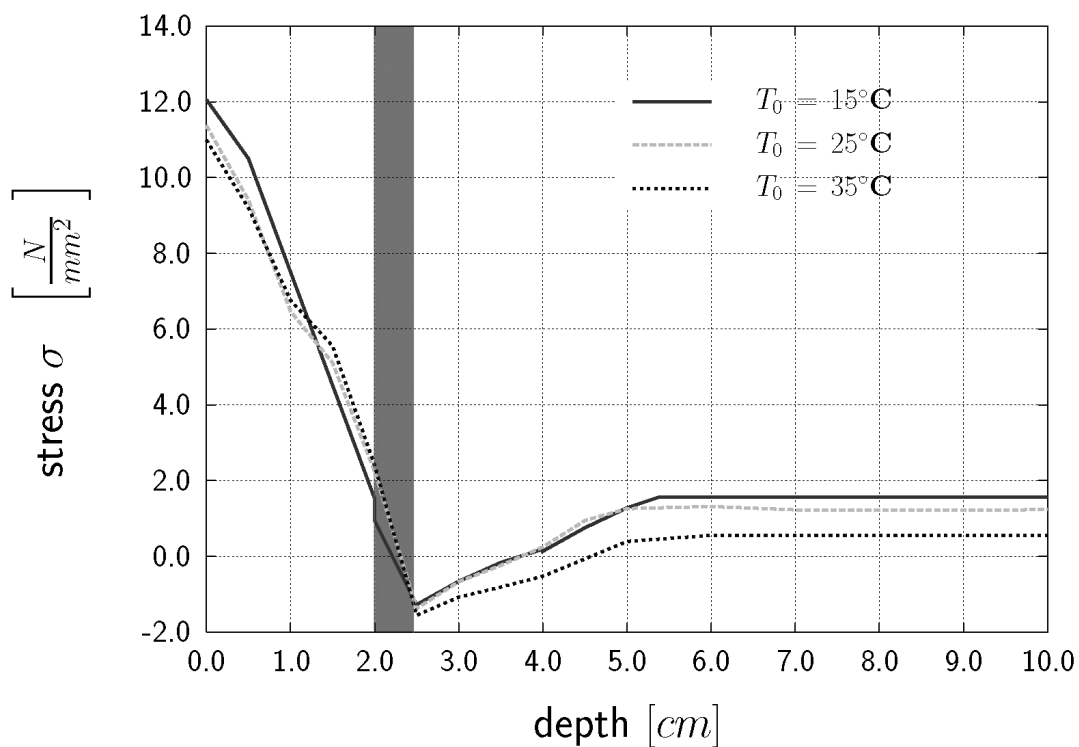


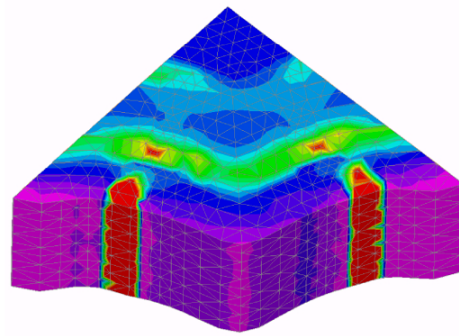
Figure 16 Influence of the reference temperature on the distribution of stresses (“thunder-shower” effect at different starting temperatures of the surface, blue = layer C consisting of 100% resin).

In another study the influence of the geometry of the specimen was investigated. The stress and strain distributions (see Fig. 17) show, that for the complex geometries (e.g. pleats or parts of the body of a sculpture) the same loading case as used before –“thunder shower”– can even cause cracks (red zones – principal strains). It can be seen that a curvatures at the surface of the specimen can lead to larger stress concentrations and therefore to crack development as well. Note that the cracks are not predefined, i.e. they occur automatically as a consequence of interaction between the thermal and the mechanical model.

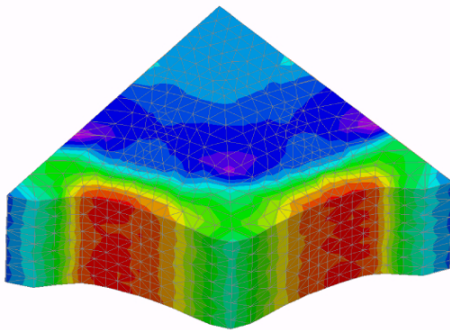
In an additional study it was found that the repeated temperature conditions (cyclic temperature loading) can cause cracking even for not extreme temperature conditions and simpler geometries.

CONCLUSIONS

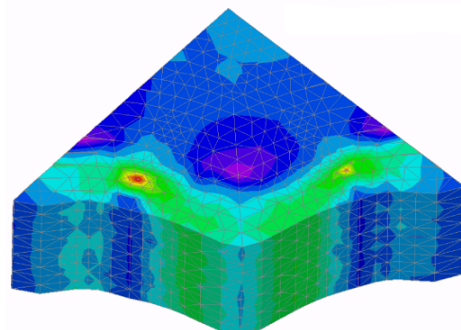
The finite element analysis based on the proposed multi-layered model indicates that large differences in the elastic properties of layers and large differences in coefficient of thermal expansion of resin-treated structure can under certain conditions cause damage (cracking). It is demonstrated that under normal climatical conditions no cracking occurs – the stresses are smaller than the material strength. However, depending on the distribution of temperature and on the geometry, in extreme cases cracking is possible. For resin-treated objects there is a danger of damage, especially if they have a complex geometries with high expanding intermediate layers of almost pure resin, like in our model the layer C. The study confirms that the finite element analysis is a useful tool to investigate the influence of the thermo-mechanical interaction on the structural response and to show the critical impacts, critical heterogenities and resulting main stresses and cracks. Moreover, the analysis can be used to select optimal material properties for conservation treatments. The results have been confirmed by experiments (see Fig 9a-c), however, further experimental and theoretical work is needed.



principal strains ε_{11} (red zones = cracks)



principal stresses σ_{11}
before the crack initiation



principal stresses σ_{11}
after the crack initiation

Figure 17 Calculated distribution of stresses and strains for the temperature distribution caused by “thunder-shower” – structure with not constant curvature, symbolising parts of a sculpture.

REFERENCES

- [1] J. Aboudi. Mechanics of composite materials: a unified micromechanical approach. Elsevier Verlag, Amsterdam, 1991, 328 S.
- [2] Z.P. Bažant, and B.-H. Oh. Crack Band Theory for Fracture of Concrete. Materials and Structures, RILEM, 93(16), 1983, 155-177.
- [3] J. Bossert. Numerische Simulation an kunstharzvollgetränkten Objekten in der Denkmalpflege – FE-Berechnungen zur thermo-mechanischen Interaktion. Diplomarbeit, Universität Stuttgart, 2003, 133S.

- [4] G. Grassegger. Die Verwitterung von Naturstein an Bauten und Bau-
denkmalern. In Naturwerkstein und Umweltschutz in der Denkmalpflege,
Ulm, 1997. Ebner Verlag, S. 433 – 490 .

- [5] J. Ožbolt. MASA - 3D Finite element program for non-linear analysis of
concrete and reinforced concrete structures. Institut für Werkstoffe im
Bauwesen, Stuttgart, 1999, 48 S.

- [6] J. Ožbolt, Y. Li and I. Kožar. Microplane model for concrete with relaxed
kinematic constraint. International Journal of Solids and Structures, (38),
2001, 2683 – 2711.

- [7] W. H. Yoon. Untersuchungen der temperatur- und feuchtebedingten
Spannungsverhältnisse im Bereich von Instandsetzungen bei massiven
Betonbauten. Dissertation, Fakultät für Bauingenieur- und Vermessung-
swesen, Aachen, 1989, 226 S.

- [8] H. Zumbroich. Einfaches Verfahren zur Ermittlung von maximalen Wär-
meeigenstressen in mehrschichtigen Außenbauteilen. Dissertation,
Fakultät für Bauingenieur- und Vermessungswesen, Aachen, 1980, 155S.

- [9] H. Zienkiewicz. Methode der finiten Elemente. Hanser Verlag, München.